Distributed and convergent representations of tools in human parietal and anterior temporal regions revealed by fMRI-RSA

Ryo Ishibashi[1], Gina Humphreys[3], Ajay Halai[3], Azumi Tanabe-Ishibashi[2], Nobuhiro Hagura[1], Matthew A. Lambon Ralph[3]

1. Center for Information and Neural Networks (CiNet), National Institute of Information and Communication Technology & Osaka University, Osaka, Japan
2. Institute of Development, Aging and Cancer, Tohoku University, Sendai, Japan
3. MRC Cognition and Brain Sciences Unit, University of Cambridge, United Kingdom

Open access: For the purpose of open access, the UKRI-funded authors have applied a Creative Commons Attribution (CC BY) licence to any Author Accepted Manuscript version arising from this submission.

Abstract

Classical models of tool knowledge and use are centred on dorsal and ventral parietal pathways. Theories of semantic cognition implicate a “hub-and-spoke” network, centred on the anterior temporal lobe (ATL), that underpins all concepts including tools. Despite their prominence, the two theoretical frameworks have never been brought together and the large discrepancy in the functional neuroanatomy addressed. We undertook a multiple-regression Representational Similarity Analysis (RSA) of task fMRI data with four (motor action, broad function, mechanical function, object structure) feature-based models. The motor action model correlated with the activation patterns in bilateral superior parietal lobules (SPL), while the models of broad function and mechanical effect aligned with the activation patterns in bilateral ATLs. The object-structure model correlated with activation patterns in bilateral middle occipital gyri. The results also showed that the ventral ATL activation patterns corresponded simultaneously with all RDM models except object structure. Furthermore, a standard univariate analysis using tool-familiarity ratings for parametric modulation revealed that the classical tool-network regions (frontal, inferior parietal, and posterior middle temporal cortices) were increasingly active as the tool familiarity reduced. These results demonstrate that parietal and ATL regions are both crucial, and motivate a major extension and revision of the neuroanatomical framework for tool use.

INTRODUCTION

The ability to understand and use tools is a crucial human ability. When it goes wrong, patients have significant disabilities and everyday challenges. Classical and contemporary frameworks for tool knowledge and use are still centred on the parietal lobe. Utilising multiple methods, convergent evidence has increasingly implicated the anterior temporal lobe (ATL) as a crucial neural area for semantic memory (including knowledge about tools). This area is, however, notable by its absence in most models of praxis and tool use. By utilising dual-echo fMRI that ensures ATL BOLD coverage and representational similarity analysis (RSA), the current paper explored, for the first time, how multiple aspects of tool knowledge are represented in the healthy brain. The results not only reinforce the importance of classical dorsal parietal regions but also heavily implicate the ATL as a major representational hub for multiple aspects of tool knowledge.

The importance of the parietal lobe for tool use was first highlighted in the 19th century via reports of stroke patients with action and pantomime deficits following parietal damage (apraxia; Jackson 1866; Liepmann 1900). The parietal lobe is now widely acknowledged as a critical cortical region for human object use, as revealed by contemporary investigations using neuropsychology, neuroimaging or stimulation methods (Boronat et al., 2005; Canessa et al., 2008; Gross & Grossman, 2008; Ishibashi et al., 2011; Pelgrims et al., 2011). Recent theories implicate two major pathways from visual to motor regions residing in the parietal lobe (Binkofski & Buxbaum, 2013; Buxbaum & Kalénine, 2010; Buxbaum & Randerath 2018). The “dorso-dorsal” pathway is located in the superior parietal lobule (SPL) and the intraparietal sulcus (IPS), and is supposed to compute object-directed actions based on the structural configuration of the object and body. The “ventro-dorsal pathway” streams from the visual MT region and runs through the inferior parietal lobule towards the supramarginal gyrus (SMG), and is argued to be important for more indirect planning of actions incorporating the known function of the objects/tools. This neuropsychologically-derived framework receives some support from fMRI which has shown that the SPL and the anterior IPS are engaged when participants make decisions about the manipulation of tools. In addition, a large number of neuroimaging studies indicate that the left SMG activates for tasks requiring tool recognition and naming (Lewis, 2006; Ishibashi et al., 2016).

In contrast to the two well-studied "dorsal" pathways, the ventral route (i.e. the temporal lobe) has received less attention in human tool use research. Though the left posterior middle temporal gyrus (pMTG) shows consistent activation in tool cognition studies, most of the anterior temporal lobe remains enigmatic (Boronat et al., 2005; Kellenbach et al., 2000; Ishibashi et al., 2016). Therefore, the human brain's "tool network" (Cabrera-Álvarez et al., 2020; Chao & Martin, 2000; Gallivan et al., 2013) often emphasizes the dorsal parietal regions

for computing praxis and the posterior portion of the left temporal cortex for the possible storage of the tool-function knowledge (Reynaud et al., 2016; Lesourd et al., 2021). There are, however, clear indications that the parietal-centric perspective may need substantial revision to incorporate more anterior temporal involvement in tool knowledge and use. First, moving beyond a parietal-stroke model, studies of semantic dementia (SD) from 20 years ago showed not only that knowledge about tools (alongside all other concepts) becomes degraded as a result of the bilateral ATL atrophy, but also that the patients become unable to demonstrate the use of these tools, with degradation of knowledge and declining tool use strongly coupled (Bozeat et al 2003). Comparisons with cortico-basal syndrome (CBS) form a double dissociation between object knowledge and motor skills, as poor knowledge and use of meaningful tools are observed in SD, while ideomotor-type dysfunction is prominent in CBS patients (Hodges et al., 1999). These patient results are mirrored by studies using repetitive transcranial magnetic stimulation (rTMS) in healthy participants (Pobric et al., 2010; Ishibashi et al., 2011) with ATL stimulation leading to transient semantic impairment for all concepts and object-function knowledge, while IPS stimulation generates poorer performance in praxis/tool-specific cognition. Despite these striking results, these past studies are limited in number and have had little impact on theoretical frameworks of tool knowledge and use, and their disorders.

Interestingly, an equivalent situation emerged in the parallel literature on the neural bases of language and its impairments. For many years, the framework for language function was built upon insights from post-stroke aphasia, which highlighted the importance of Wernicke's and Broca's regions and the dorsal pathways between them (though see Weiller et al., 2011). Over the past twenty years, convergent data from functional MRI, cortical electrode explorations, TMS, computational modelling and semantic dementia studies have extended these language frameworks to include ventral pathways and key regions such as the ATL (Ueno et al., 2014; Saur et al., 2008; Lambon Ralph et al., 2017; Mesulam, 2023; Shimotake et al., 2015). Accordingly, the central thesis of this paper is that an equivalent, significant expansion of the framework for human praxis is overdue.

Motivated by these lines of research, we investigated how neural encoding tool-representations extends beyond the parietal-centric regions in neurologically healthy brains. We were especially interested in whether the more anterior parts of temporal lobes are involved in representing any aspects of tool information. The current study made use of two critical technical developments. First, multi-echo EPI techniques for fMRI improve sensitivity within the ATL, which is challenged by multiple factors including its higher magnetic-susceptibility artefact (Halai et al., 2014; Poser and Norris, 2009; Poser et al., 2006; Visser et al., 2009). Secondly, Representational Similarity Analysis (RSA) allows the researcher to go

beyond univariate analysis to investigate local neural coding of different types of representations from their multi-voxel pattens of activation. We used these opportunities to tackle, for the first time, the following questions: (a) which brain regions are implicated in different aspects of tool knowledge such as the body movements for use and their functions (whole-brain analysis); (b) which aspects of tool knowledge are represented in the classical parietal-centred 'tool-network' regions (i.e. SPL, SMG and pMTG) and which aspects of tool knowledge, if any, are supported by the ATL (region-of-interest analyses); and (c) are there any areas that integrate multiple types of different tool information? Our findings reveal that (*a*) superior parietal (SPL) and anterior temporal (ATL) regions predominantly represent tool "action" and "function" information, respectively; (*b*) except for the SPL, the classical tool-network regions (i.e. SMG and pMTG) do not correlate with any of the examined tool information; and (*c*) the ventral part of ATL, the acknowledged "semantic hub" region, integrates various tool-relevant information including both function and action knowledge. In addition, our data revealed that (*d*) the activation in tool network increases for less common tools, with the activation pattern exhibiting significant overlap with the semantic-control network observed in our previous studies.

These findings are in alignment with the semantic hub-and-spoke model where the ATL 'hub' area combine information from other modality-specific 'spoke' regions in the brain (Lambon Ralph et al., 2017). Considering SPL as the essential spoke area for processing the motor actions, the current results draw out the comprehensive tool-representative network on the firm ground of the recent information-based analysis of brain activations for the recognition and use of common tools.

RESULTS

Functional-MRI Results: Whole-brain searchlight analysis and ROI analysis

The analysed data were collected in a tool-viewing fMRI experiment designed for this study. Ninety colour photographs depicting familiar tools (mechanical tools, office/kitchen utensils, gardening tools, and personal grooming items) were presented to participants during the fMRI scan (Fig. 1-A). They judged whether each tool is typically used indoors or outdoors. This task served two purposes: 1) to prevent participants from falling asleep during the scan and 2) to ensure that the task decision was orthogonal to the tool-information models used in the Representational Similarity Analysis (RSA). They also rated familiarity of the tools on a 5-point Likert scale (1 = not familiar at all, 5 = very familiar) after scanning. We employed a multi-regression RSA approach (Kriegeskorte et al., 2008; Nili et al., 2014; Tucciarelli et al., 2019). Four models were used to represent different types of tool information: broad function (bF), mechanical function (mF), motor action (A), and object structure (Str). The models were created based on a normative object use feature study which was part of a previous investigation of tool knowledge in patients with semantic dementia (Bozeat et al., 2002). The broad-function model encodes the possible situations that the tools can be used in (e.g., gardening, cooking, etc.). The mechanical-function model includes features of the mechanical purpose each tool can be used for (e.g., cutting, making a hole, etc.). The motor-action model consists of the elements of hand and arm movements when using each tool (e.g., gripping, pinching, striking down, etc.). The object-structure model consists of the visible structural properties of the tool (e.g., rod-shaped, round-shaped, having a joint, etc.). This last model was expected to serve as a 'control' model to validate the analytical methods by examining the visuo-perceptual representation in visual cortex. For each of the four models, representational dissimilarity matrices (RDMs) were calculated and used as predictors of corresponding dissimilarities in neural activation patterns. We used searchlight method with a mixed-effect multiple regression model including all the four predictors. Analytic procedure for the whole-brain searchlight analysis is illustrated in Fig.1-B. The region of interest (ROI) analysis was conducted in the same way, except that limited number of anatomically defined ROIs were used to calculate neural RDMs. See Methods for further details of the experimental procedures and the precise pipeline of the analysis.

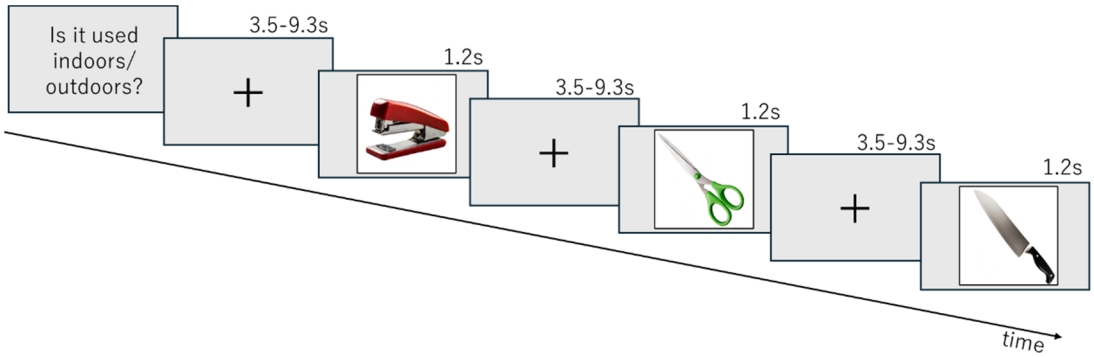

Figure 1-A. Schematic image of the behavioural task within the scanner.

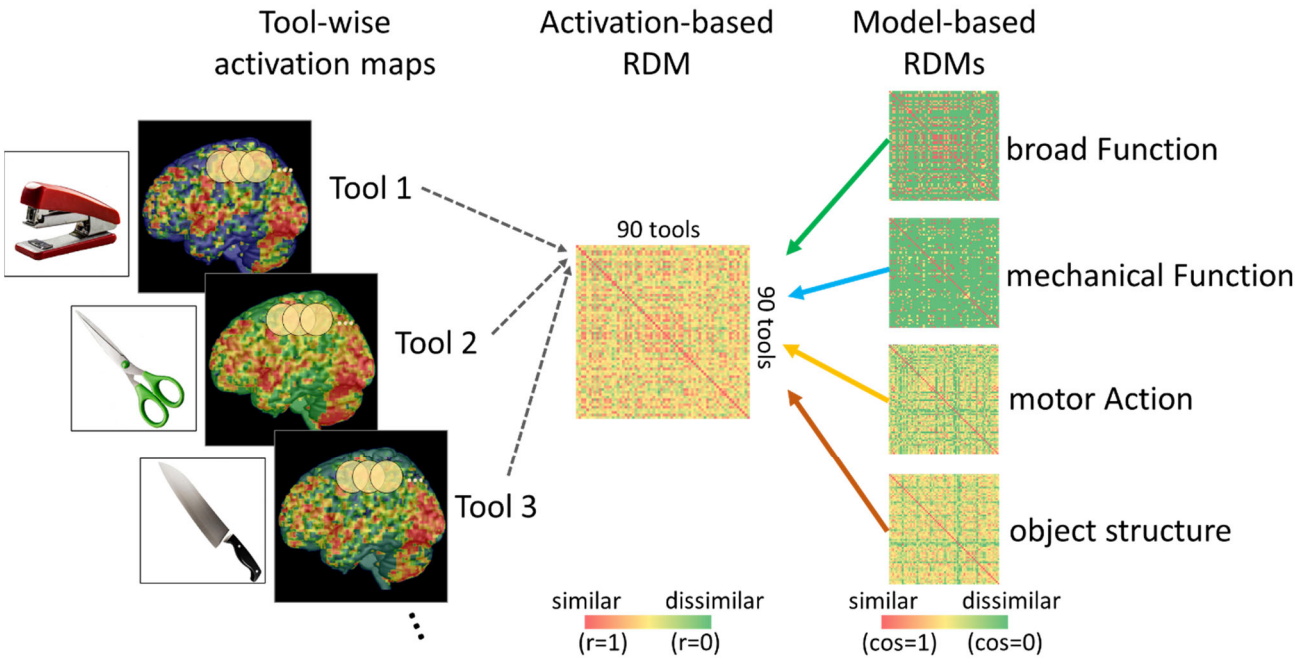

Figure 1-B. Illustration of a multiple-regression RSA step for a given searchlight. The estimated standardized regression coefficients were recorded for the location (centre) of the searchlight. Note that the actual analysis was conducted on the combined activation-based RDMs from all the participants. This mixed-effect regression analysis was repeated moving the searchlight across the whole brain to yield the coefficient map for each model.

Fig.2 shows the results of the whole-brain searchlight analysis. The two function-knowledge model, broad-function as indicated in green and mechanical-function shown in light blue, had high correlations mostly within the bilateral temporal lobes, with largest clusters at the anterior temporal lobes. The motor-action model (yellow) highlighted some parietal areas including bilateral superior parietal lobules and the right inferior parietal lobule.

It also had high correlation with the activation patterns in the right inferior temporal gyrus and the left ATL. The object-structure model had high correlation in the bilateral occipital regions, roughly corresponding to the secondary visual cortex. The local maxima of the significant clusters for the four feature models are listed in Supplementary Tables 1A-D.

The ROI analyses built on the searchlight results and allowed us to focus on key areas implicated in the classical praxis frameworks as well as the hub-and-spoke semantic model. Fig.3 show the results of the ROI analyses, dividing the ROIs by existence/absence of a significant effect of any of the four models. Fig.3-A shows that bilateral SPLs (involving the upper bank of IPS) had significant similarities with the motor-action model, the ATLs had correspondence with broad-/mechanical-function models, and the middle occipital gyri activates in high similarity with the object-structure model. The right SMG also had a significant correspondence with the structure model. The left SMG and the bilateral pMTGs, as indicated in Fig.3-B, had no significant similarity in their activation patterns with any of the four feature models.

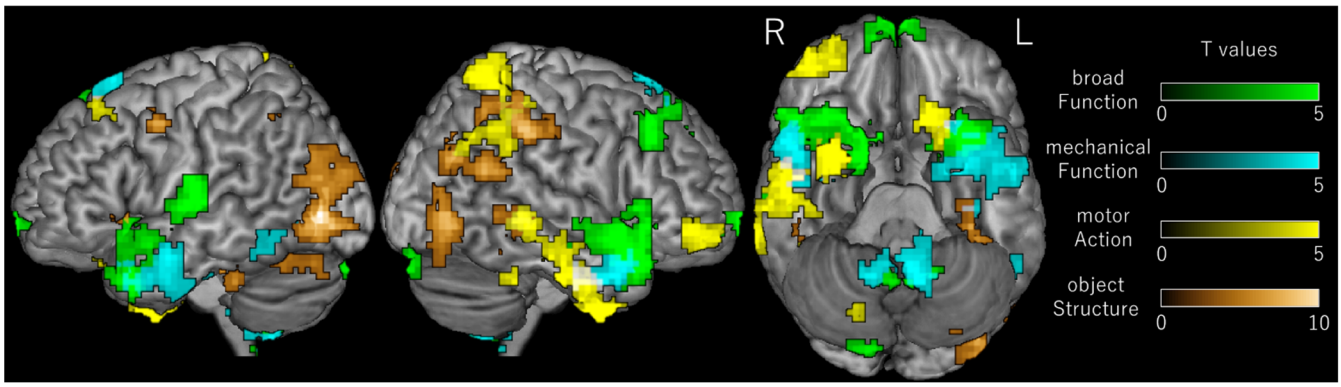

Figure 2. Results of the whole-brain searchlight analysis. Voxel-wise threshold was set at uncorrected $p<0.001$. Cluster-extent threshold was applied for each model map with an FDR-corrected threshold for $p<.05$. The minimum size of significant cluster was 43, 46, 49, and 42 voxels for the broad-function, mechanical-function, motor-action, and object-structure models, respectively.

While the strongest contrast was observed between action and function models, the distribution of the significant clusters for each model gives important additional insights. Motor-action information was not exclusively represented in the parietal regions of the brain, but also represented in the bilateral temporal lobes. Some bilateral temporal areas also showed similarity to the motor-action model, making anterior parts of bilateral ATL the most probable overlapping areas across models. Accordingly, we conducted a conjunction analysis to confirm if any area represents both function and action types of tool knowledge (i.e., similarity to the first three models). Four clusters were found significant (Fig.4-A, Supplementary Table 2).

The largest cluster locates within the left ATL extending into left inferior frontal gyrus (see Fig.4-B for the confirmation of regression results at the peak-ATL searchlight). The right ITG (covering the caudal ATL and fusiform gyrus), left insula and cerebellum were also detected as showing significantly similar activation patterns across the three tool-knowledge models.

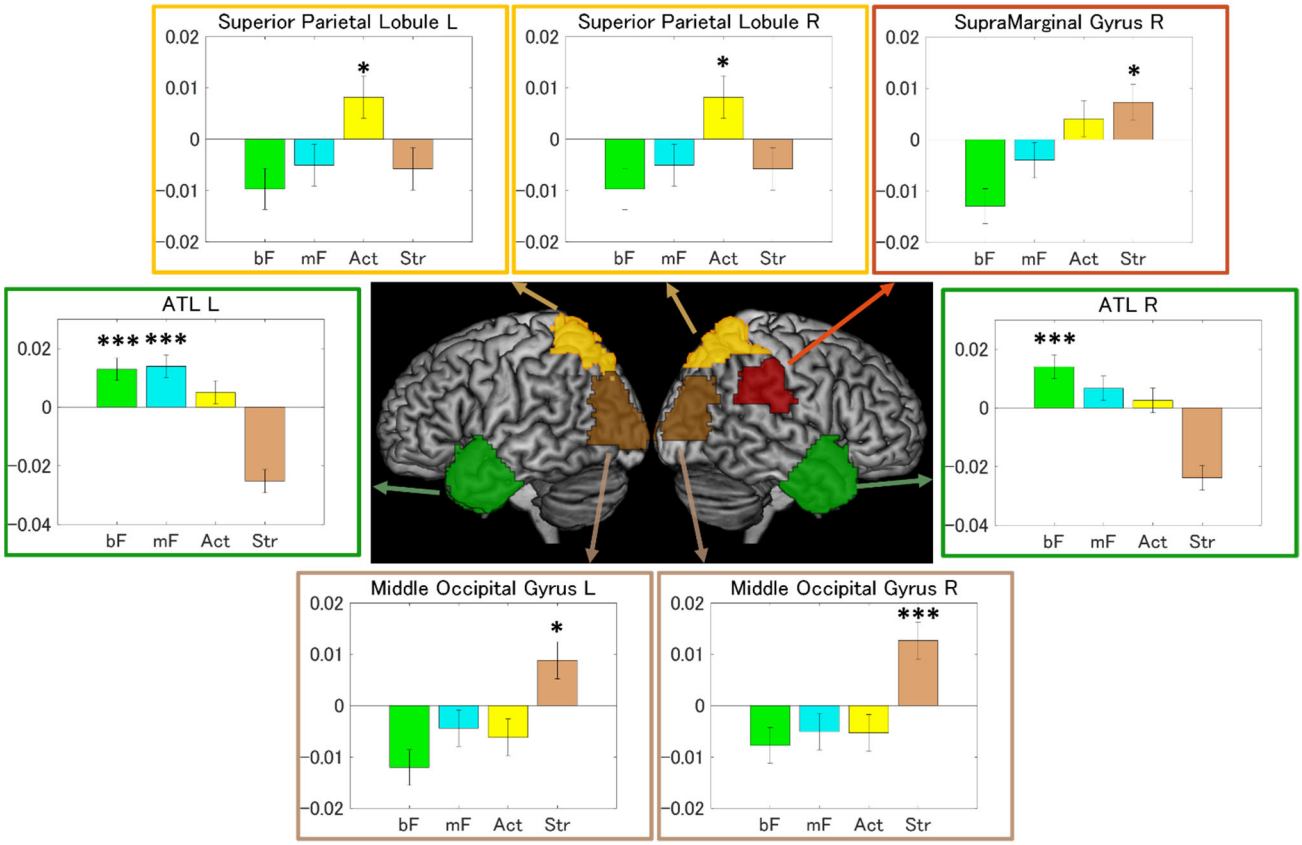

Figure 3-A. Regression coefficients for anatomical ROIs with significant positive effect by at least one of the four models. (bF: broad function, mF: mechanical function, Act: motor action, Str: object structure. ***:p<.001, **:p<.01.*:p<.05)

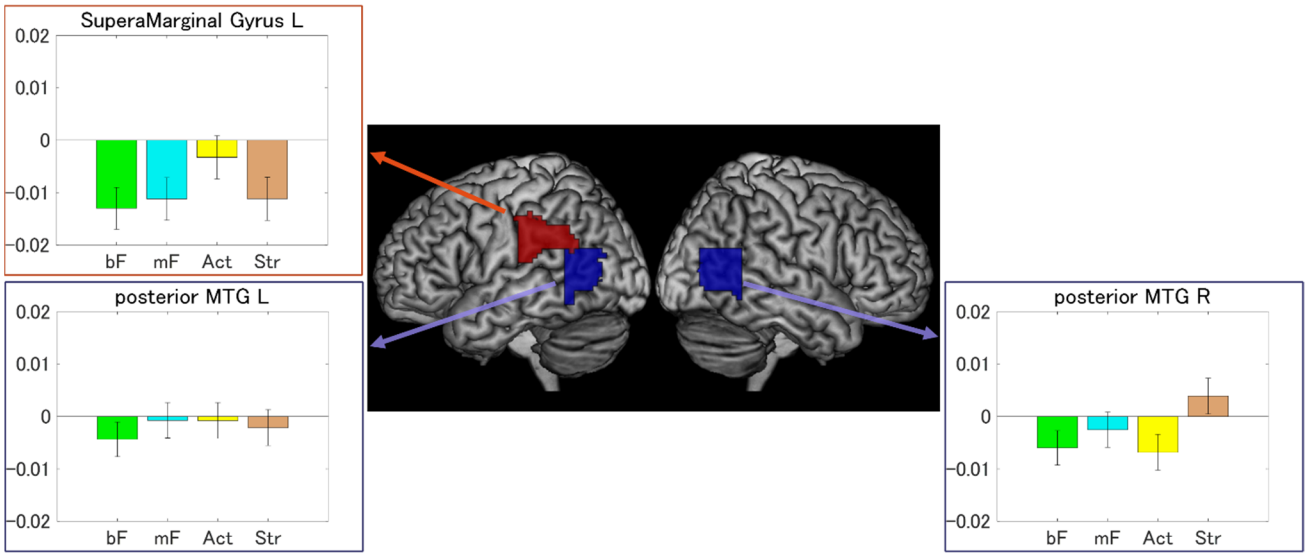

Figure3-B. Regression coefficients for anatomical ROIs with no significant positive effect by any of the four models. (bF: broad function, mF: mechanical function, Act: motor action, Str: object structure. All ps>.05)

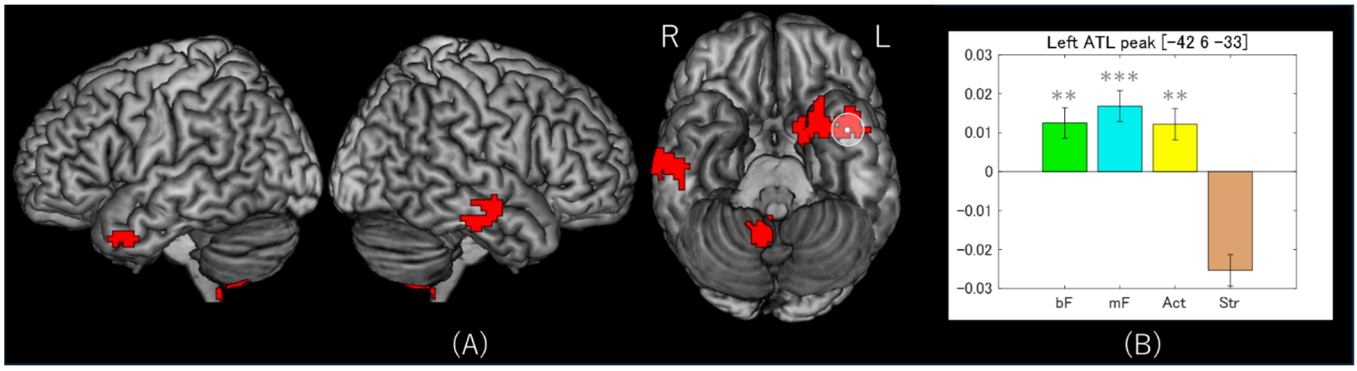

Figure 4. A) Areas with representational similarities to all three types of tool information. Cluster-extent threshold was applied for each cluster with the FDR-corrected threshold for p<.05. The minimum size of significant cluster was 39 voxels. The white dot and circle indicate the location of the voxel with the peak T value and its corresponding searchlight in the left ventral ATL. B). Estimated weights of the four regressors at the peak searchlight from the conjunction analysis. Grey stars at the top indicate the level of statistical significance. Note that significant tendency at the level of p<.10 is obvious for the first three regressors by the nature of this analysis. The bar plot and the statistical results are presented here for confirmatory purpose. ***: p<.001, **: p<.01
bF: broad function, mF: mechanical function, Act: motor action, Str: object structure.

Functional-MRI Results: effects of tool familiarity across the tool-network activation

The univariate task-related activations (Fig. 5-A top row, left) revealed the typical fronto-parietal and occipito-temporal 'tool-network' areas found in previous studies and ALE meta-analyses (Chao & Martin. 2000; Federico et al., 2023; Ishibashi et al., 2016; Lewis 2006; Wang et al., 2018). These same areas were also observed in the map of areas where activation correlated with the degree of unfamiliarity with each tool (i.e. more activation for less familiar tools; Fig. 5A second row, left). As these same areas have been implicated in semantic-executive control, we compared them directly with the results from previous work on semantic and domain-general control (Humphreys et al., 2017). There was striking resemblance including the left pMTG/occipito-temporal cortex, SMG, and bilateral frontal/prefrontal regions (Fig. 5-B, left). The overlap in the posterior pMTG also corresponded to the location of common activation for semantic activation and tool cognition indicated by a recent large-scale meta-analysis (Hodgson et al., 2023; Fig.5-B in the enlarged view).

The reverse contrasts indicated that the regions positively correlated with tool familiarity were the dorsal medial prefrontal cortex (mPFC), posterior cingulate cortex (PCC), and bilateral angular gyri (AG) —typical task-negative areas which deactivate in various cognitive tasks, including the current fMRI task (Fig. 5-A right). There were also some familiarity-correlated activations in bilateral lateral ATLs, which are also sometimes a subcomponent of the task-negative network (Buckner et al., 2008; 2019; Jackson et al., 2019; Menon et al., 2023) and tend to show enhanced deactivation in line with increasing task demands (Humphreys et al., 2015). In line with this result, there was a strong correspondence (Fig. 5-B, right) of the familiarity-positive activation correlation map from this study with the task-negative activation for non-semantic tasks observed in a previous multi-experiment study (Humphreys et al., 2015), including overlap in the medial prefrontal-parietal regions (mPFC, PCC), bilateral AG, and bilateral lateral ATLs.

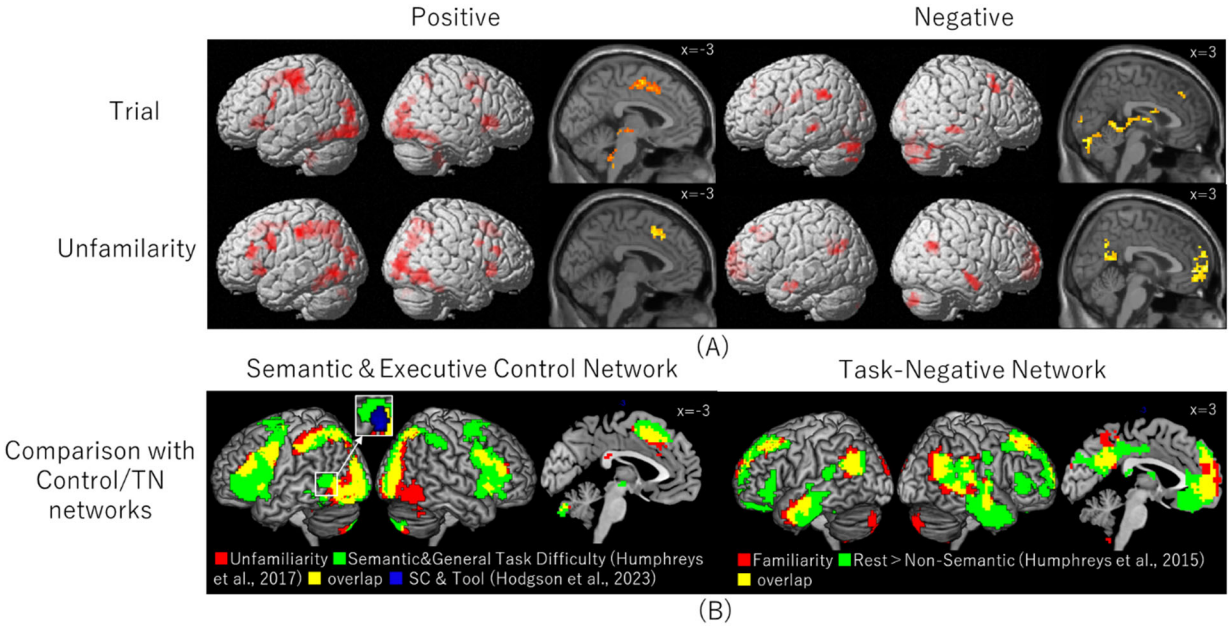

Figure 5. Mass-univariate activation maps. A) task-related base activation (top) and its parametric modulation by unfamiliarity of the presented tool (bottom); B) Overlays of the parametric modulation maps with other results from previous studies on general/semantic executive demands (left) and on the task-negative activation.
Maps in panel A are all thresholded at a cluster-forming threshold of $p<.001$ and then small clusters were removed based on FWE-corrected cluster-extent threshold of $p<.05$. In panel B, the activation maps were thresholded at $p<.05$ for exploratory purpose. The Rest>Non-Semantic contrast was thresholded at $p<.005$ for its relatively large sample size (N=69). Clusters smaller than 25-voxel size are not shown for the sake of brevity. TN: Task-Negative.

DISCUSSION

Classical and contemporary frameworks for tool knowledge and use are still centred on the parietal lobe. By utilising contemporary fMRI acquisition methods and analytics, the current study was able to investigate, for the first time, how multiple aspects of tool knowledge are represented in the healthy brain. The results not only reinforce the importance of classical dorsal parietal regions in human praxis but also heavily implicate the ATL as a major representational hub for multiple aspects of tool knowledge, and suggest that a significant extension of the classical model of object use is necessary; changes that parallel those found in contemporary models of language and semantics. We consider below how the relationship of the current results to: (i) classical models of praxis in the dorsal parietal cortex; (ii) the striking multifaceted contributions of the ATL to tool knowledge and use; and (iii) the role of posterior lateral temporal and inferior parietal regions in object tool use.

SPL and the dorso-dorsal pathway: Consistent with the classical dual-route theory, we found that SPL/IPS activation was correlated with the motor action RDM. This region is known as the where/how pathway in visual information processing, and is thought to perform planning of hand-object interactions from visual information (Goodale & Milner, 1992; Goodale et al. 2005). Cortical damage in SPL/IPS causes deficient object-directed actions including dysfunctional reaching and grasping (Binkofski et al., 1998; Cavina-Pratesi et al., 2013; Karnath & Perenin, 2005; Perenin & Vighetto, 1988). As the motor action RDM consists of features of the grip and arm movements for tool use, the present results suggest that body-movement for tool use is indeed calculated/represented in the bilateral SPL/IPS regions. Corroborating this view, a recent study found successful decoding of planned grasp type from activation in both right and left anterior IPS (Michalowski et al., 2022), and activity in bilateral IPS during planning tool-use has been found to increase with the complexity of manipulating each tool (Ras et al., 2022). Some clinical studies also suggest that the SPL contributes tool-manipulation knowledge, as SPL-damaged patients struggle to show canonical manipulation of common tools without agnosia on the tools (Valério et al., 2021; Peigneux et al., 2001).

The importance of the ATL semantic hub: perhaps the most striking aspect of the current study was the importance of the ATL in the representation not only of two forms of tool function knowledge but also of motor actions (indeed, only visual form similarity did not engage the ATL). Furthermore, the ATL was also one of the only regions that jointly represented these three different aspects of tool knowledge. Though the ATLs have never been explicitly integrated into the models of human tool use, our results provide clear evidence that the integration is necessary; in the same way that the ATL has been integrated into

contemporary models of language and semantics (Chen et al., 2017; Frisby et al., 2022; Lambon Ralph et al., 2017; Mesulam, 2023; Patterson et al., 2007). The absence of the ATLs from models of praxis (and previously language) probably reflects the neuropsychological origins of the classical models which were founded on the study of patients after MCA stroke. The middle-to-inferior aspects of the ATLs are in the watershed between the MCA and PCA (Lambon Ralph et al., 2017; Phan et al., 2005; Zhao et al., 2020), and thus unlikely to be damaged after embolic stroke (and even less likely to produce bilateral ATL damage, which is the atrophy distribution in semantic dementia: Ding et al., 2020; Rouse et al., 2024). The RSA results fit precisely with previous investigations of ATL and IPL using TMS (Ishibashi et al., 2011: Pobric et al., 2010) and most directly with past explorations of tool knowledge and use in SD patients, which showed parallel degradation of semantic knowledge of tools (as a part of their generalised semantic deficits) and impaired object use (Bozeat et al., 2000; 2002; Coccia et al., 2004; Hodges et al., 1999; 2000).

The discovery of ATL involvement in tool-representation is also consistent with the semantic hub-and-spoke model of semantic cognition (Lambon Ralph, 2017). The framework posits that the bilateral ATLs serve as a modality-general 'hub', integrating multimodal information over time to build generalisable conceptual knowledge (Lambon Ralph et al., 2010; Jackson et al., 2021). Indeed, the convergence of multiple forms of tool knowledge into the ATL also fits with recent decoding results from cortical grid electrode recordings which showed that the ATL does not simply represent various semantic dimensions separately but actually encodes them simultaneously to form a unified semantic space (Cox et al., 2024).

Neuroanatomically, ATL involvement in praxis may also seem somewhat surprising given its distance from other tool-related cortical areas. Although the cortical distances between ATL and SPL are large (almost as large as they can be within the same hemisphere), they have direct white-matter connectivity allowing fast, efficient communication and emergent functional interactions. Human and non-human primate tractography studies have found that the superior ATL and inferior parietal cortices are connected along the middle longitudinal fasciculus (Menjot de Champfleur et al., 2013), then extending beyond AG up to the SPL (Wang et al., 2013; Markis et al., 2013). In parallel, the inferior longitudinal fasciculus (ILF) not only connects the temporal pole with occipital visual areas (Tusa & Ungerleider, 1985; Catani et al., 2003) but also branches at the ventral occipito-temporal area to ascend, medially, into the dorsal parietal cortex, in both non-human primates (Selzer & Panja 1984; Schmahmann & Pandya, 2009) and humans (Lang et al., 2017). Whether this ascending parietal branch should be regarded a part of ILF remain controversial (Mandonnet et al., 2018; Bullock et al., 2022), however it is quite possible that neurons in the SPL and ATL are connected directly via midLF, or through a single intermediating region at the occipito-

temporal region.

Temporoparietal and ventro-dorsal pathway contributions: The null RSA results for the left pMTG and SMG are potentially puzzling given that these regions are frequently noted in tool-use/recognition (univariate) fMRI studies, as well as being a key area of damage in ideational apraxia (Goldenberg & Spatt, 2009; Goldenberg & Randerath, 2015; Hodgson et al., 2023; Ishibashi et al., 2016). There are at least two possible explanations. The first is insufficient statistical power in the MVPA analysis, although the additional univariate analysis with the same data revealed two important findings: (1) both the pMTG and SMG were activated by the tool decision task, and (2) these two regions, along with the inferior frontal gyrus (IFG), responded more strongly to the least familiar tools. In keeping with these results, the second possible explanation is that these regions (along with PFC) support semantic control (Jackson et al., 2021; Jackson, 2021; Lambon Ralph et al., 2017); a conclusion supported by convergent evidence from fMRI, rTMS and neuropsychology (Hallam et al., 2016; Jefferies, 2013; Whiteney et al., 2011; 2012). In fact, patients with damage to these brain regions not only show multimodal semantic control deficits (semantic aphasia: Jefferies & Lambon Ralph, 2006; Jefferies et al., 2008; Noonan et al., 2013; Thompson et al., 2022) but also present with ideational apraxia (Corbett et al., 2009a, 2009b; 2011; 2015).

The reason why tool cognition and semantic control align in these same regions (see Fig. 5; and also recent large-scale ALE examinations: Hodgson et al., 2023) is not fully understood. It is possible that some executive planning is required or automatically triggered in the recognition of tools. Multiple recent reviews on the neural mechanisms of human tool use argue that tool use is not simply the recall of movement information stored for each tool, but rather a compositional process for integrating relevant physical information of the tool and expected target objects for a desired goal state (technical-reasoning hypothesis; Jarry et al., 2013; Osiurak & Badets, 2016; Lesourd et al., 2021). Although this account has focussed on the role of left SMG, the required executive process for tool-use 'reasoning' is likely to require contributions from multiple multi-demand and semantic control areas beyond SMG alone.

Conclusion: the adoption of RSA and multi-echo fMRI shows that the cortical areas implicated in human tool cognition and use go beyond the classical parietal-centric dorso-dorsal and ventro-dorsal pathways. A more comprehensive account is needed, in which the classical framework is extended to include the ATLs' essential role in representation of multiple aspects of tool knowledge, plus the support of the FTP semantic-control network for controlled, goal-directed tool-use actions.

METHODS

Materials

We based our selection of tool stimuli on the neuropsychological study by Bozeat et al. (2002). The study examined tool-relevant cognitive performance of patients with semantic dementia utilizing a set of 90 different tools. We collected visual photo images of the corresponding 90 tools and used them for the present experiment (see Supplementary Table 3). Each collected image was converted to a 24-bit bmp file and then scaled to fit into the same image dimensions (400 × 300 pixels) using Windows Paint software.

Participants

We recruited 22 graduate/undergraduate students in the University of Manchester. Their age range was 18-30 years (Mean 21.9; SD = 3.2). All had normal or corrected-to-normal vision and were right-handed (mean score in Edinburgh Handedness Inventory was +89.0). They gave their informed consent before taking part in this study and were reimbursed for their time. Two of them had to cancel their participation during the experiment (one at their will, another for a technical problem with the MRI scanner). Data from another participant had irreversible error (mixed-up slices) detected right after the recording. We therefore used data from the other 19 participants in the following analyses.

Experimental Procedure

Participants were engaged in visual recognition of tools while lying supine in the MRI scanner (Fig.1). The stimuli were presented with a projector system and seen in a mirror attached to the head coil. To make sure that the participants attend to the meaning of each stimulus, they were asked to judge whether the tool is used indoors or outdoors, and reported their decisions by pressing a button on a response box in their right hand. The responses were made using their right index and middle fingers. The assignment of buttons to the two (indoor/outdoor) categories was counterbalanced across participants. Each of the 90 stimuli appeared only once in a session and stayed on the screen for 1.2 seconds regardless of their responses. A fixation cross on a grey background was presented when no stimulus is presented. The interval time between stimulus presentations were determined in advance using Optseq program (Dale, 1999; https://surfer.nmr.mgh.harvard.edu/optseq/) for each session. The intervals were set to range between 3.5-9.3 seconds by the minimum steps of 250ms and to have the mean of 4.8 seconds. The average stimulus onset asymmetry (SoA) was hence 6.0 seconds. A 16-second interval was added at the beginning and the end of each session to accommodate extra margins for the baseline. We used E-Prime software (Psychology Software Tools inc.) to implement the presentation of stimuli and the recording of the participants' responses.

Participants performed the task in 5 sessions (approximately 55 minutes in total with in-

scanner breaks between sessions) with functional scanning, following an initial scanning of the structural T1 data of their brain (about 5 minutes). Before entering the scanner, they practised the task on a laptop PC. All stimuli appeared just once in the practice session with the tool name shown below the image. This was to enhance their correct recognition of these images. After all sessions in MRI scanner, the participants were asked to provide a familiarity rating for each tool on a Likert scale between 1 ("not at all") and 5 ("very"). This rating task was conducted to confirm the familiarity of the tools across participants and to establish inclusion/exclusion of the tools in the main analysis: only tools with a familiarity rating>4.0 (on average) were included in the later RSA analysis in order to ensure that representational analyses were based on items that participants knew well. The rating resulted in 22 of 90 items having the mean familiarity <4.0. We used all items in a subsequent parametric-modulation analysis of the effect of familiarity in these task fMRI data (see below). The accuracy of the indoor/outdoor judgments on the included 68 items (58 indoor, 10 outdoor tools) was very high: 91.8% (SD=2.8). The mean response time was 749.9ms (SD=48.6).

Image Acquisition with Dual-Echo fMRI sequence

We used a dual-echo sequence with 12ms and 35ms echo times for data acquisition (Halai et al., 2014; 2015). This method helps to reduce the effect of signal-dropouts at the basal parts of anterior temporal lobes and orbitofrontal cortex. Because tissues with heterogeneous magnetic susceptibility (e.g. cortex, bone, air) lie in close vicinity in these areas, canonical fMRI protocols with single echo time of around 35ms create large distortions in these regions. Given that signal dropout increases with echo time, the shorter of the dual echoes provides better signal recovery in these challenging areas, whilst the greater SNR of the longer echo time for other brain areas is retained (Halai et al., 2014; 2015). Thus we adopted this acquisition method for our experiment.

Preprocessing

The preprocessing steps followed the method established in previous dual-echo fMRI studies (Halai et al., 2014; 2015). The short-echo and long-echo images were re-aligned to the first volume in each session and then the signals were combined using a simple average at each voxel. The combined data were then passed to the subsequent pre-processing steps on the Statistical Parametric Mapping software (SPM8, https://www.fil.ion.ucl.ac.uk/spm/), which included slice-timing correction to the first (bottom) slice in each volume, coregistration of the first EPI volume with individual T1 image, and normalisation using DARTEL algorithm (Ashburner, 2007). No smoothing was applied to the data as the main purpose of this study is to explore multi-voxel patterns.

Preparation for RSA: Univariate Analysis for Estimating Tool-Wise Activation Patterns

Voxel-wise GLM analysis was conducted using SPM8. We adopted a Condition-Rich

design (Kriegeskorte et al., 2008) to model the BOLD signals at each voxel, setting each of the 90 stimulus as a different condition. Participants' key-presses were modelled as an additional single 'responses' condition. Six volume-realignment parameters (6 parameters) from the preprocessing were also added to regress out the head-motion noise. We also applied a high-pass filter of 128 seconds to remove low-frequency noise at each voxel. After estimating weights for all regressors, we calculated subject-wise contrast images for each of the 90 stimuli versus implicit rest. Excluding activation maps for the low-familiarity tools, a set of 68 × 19 contrast images were created as the target data for the following RSA analysis.

Multi-Voxel RSA with Linear Mixed-Effect Regression

We adopted a multi-regression RSA approach (Kriegeskorte et al., 2008; Nili et al., 2014; Tucciarelli et al., 2019). Four models were used to represent different types of tool information: broad function (bF), mechanical function (mF), motor action (A), and object structure (Str). The models were created based on a normative object use feature study which was part of a previous study on investigation of tool knowledge in patients with semantic dementia (Bozeat et al., 2002). These models consisted of codes on the existence (1) or absence (0) of certain features on each of the 90 tool stimuli, providing a binary-code vector for each tool concept. The "broad function" of tools indicated the possible situations each tool can be used in. The "mechanical function" model (mF) involves a short description of mechanical purpose which each tool can be used for. The "motor action" model consists of the types of hand and arm movements involved in using each tool. The "object structure" model consists of visible structural properties of the tool. For each of the four models, cosine similarity was calculated for each pair of tools and then 1-cos was used as the model's representational dissimilarity matrix (RDM). The object structure model was involved in the analysis as a 'control' regressor. It was expected to prove the quality of the data and validity of the analytical procedure by showing high correlation in the occipital visual cortex.

We conducted both whole-brain and region-of-interest (ROI) analyses. In the whole brain analysis, we used a searchlight method with a linear mixed effect model (LME) analysis. The group-level mask image calculated from DARTEL processing was used as the area to explore. A spherical searchlight with 9mm radius (involving 123 voxels) around each voxel was used to extract the multi-voxel patterns. Pearson's correlation coefficients (r) across the tool stimuli were calculated and 1-r was used as the activity-based RDM. We conducted a mixed effect multiple-regression analysis with the upper triangular part of the activation-based RDM as the dependent variable and those of model RDMs as explanatory variables (see Fig.2). Weighting of the four regressors were thus estimated for each searchlight location. This step was repeated for the search light across the whole brain. We created four T-value maps for the four model regressors, truncated them with uncorrected voxel-wise threshold of $p<.001$ and

applied cluster-extent thresholding of $p<.05$ corrected for FDR to detect significant clusters. Only positive values were mapped and considered legitimate targets of significance tests in this RSA.

In the ROI analysis, we examined five anatomical ROIs in both hemispheres: two ROIs in parietal lobe (SPL, SMG), two in temporal lobe (ATL, pMTG), and one at the middle occipital gyrus (MOG). The parietal ROIs were chosen as the representative parts in the dorsal (dorso-dorsal and ventro-dorsal)pathways and the temporal ROIs as the representative parts along the ventral pathway. The MOG was chosen as a control region to examine the correspondence between low-level visual features (i.e. object-structure model) and the activation patterns in the visual cortex. We used WFU pick atlas (Maldjian et al., 2003) and AAL3 (Rolls et al., 2020) toolboxes to define four of the five ROIs. The ATL mask for a previous meta-analysis for temporal-lobe activation in fMRI studies (Rice et al., 2015) was utilised as the ATL-ROI. Regression analysis was conducted on the activation-based RDMs in each ROI. As in our searchlight analysis, only positive weights were considered targets of significance tests in this analysis.

Following these two analyses, we also conducted a conjunction analysis on the results of the models in the searchlight analysis. As we were interested in where the various semantic components are combined, the conjunction analysis was applied for the results of the first three models excluding the object structure (i.e., broad function, mechanical function and motor action) excluding the control model (object structure). The three T-maps were combined taking the minimum T statistics at each voxel. Significance tests were performed the same way as in the searchlight analysis. A voxel-wise threshold of $\alpha <.001$ was first applied on each voxel (equivalent to $p<.001$ for the combined T map, i.e. $p<.10$ for each model). Cluster-extent threshold of $p<.05$ was then applied with FDR correction for the number of detected clusters.

Univariate Analysis with Tool-Familiarity as Parametric Modulator

To examine the general task-related activation in this study and its correlation with the level of the participants' tool knowledge (i.e., rated familiarity on the stimuli), we also conducted a univariate activation analysis on the same pre-processed data using each tool's mean familiarity as a parametric modulator. All tool-presentation events were combined into a single "Stimulus" condition. Stimulus-wise mean familiarity values were added into the design matrix as a parametric modulator of the stimulus-evoked activation. The participants' key-presses were also included in the model as a regressor of no interest. Both positive and negative contrasts were calculated for the base activation (task-positive/task-negative) maps and for the parametric-modulation (familiarity-/unfamiliarity-correlated) maps. The group-level activation maps were computed for each contrast and voxel-wise significance was tested

using one-sample t test. Images were thresholded at a cluster-forming threshold of $p<.001$ and then small clusters were removed based on FWE-corrected cluster-extent threshold of $p<.05$. The results were compared with the results of our previous fMRI/meta-analysis studies reporting Semantic-/Executive-Control and Task-Negative networks (see also the caption of Fig.5).

Acknowledgment

This study was supported by JSPS Overseas Research Fellowship to RI (H27-612), an MRC Career Development Award to AH (MR/V031481), an MRC Programme grant to MALR (MR/R023883/1) and an intramural award (MC_UU_00005/18).

Notes on FWHM estimation:

The FWHM for cluster-extent thresholding was estimated based on a simulation of spatial auto-correlation between neighbouring voxels. We utilised the ratio of shared number of voxels between two neighbouring searchlights in the current setting (94 of 123 voxels in a single searchlight). On a MATLAB-R2022b platform, we first generated random Gaussian noise in an array of 123 × 68 cells. For each array, 29 × 68 cells were updated by another Gaussian-noise simulation keeping 94 × 68 of them unchanged. The 68-by-68 RDM was calculated for the original and the updated arrays, and then the upper-triangle part was extracted as a vector from each. These steps were repeated 19 times to simulate the noise data from 19 virtual participants. Then, the vectors were concatenated to create a single error vector for the original and updated vectors, respectively. This was to simulate the number of datapoints for the current multiple-regression RSA. The correlation between the original and updated error vectors were then calculated as an index of simulated pure-noise-based autocorrelation between a pair of neighbouring searchlights. The entire above procedure was repeated 10,000 times to simulate distribution of correlation values in multiple pairs of searchlights, and the average r=0.761 (SD=0.0031) was taken as the theoretical spatial autocorrelation between neighbouring datapoints in the current whole-brain analysis. The in-house script for this simulation is available upon request to the corresponding author.

Supplementary materials

Supplementary Table 1: Clusters with significant extent with p<.05 corrected for the number of detected clusters. Labelling is based on AAL3 atlas (Rolls et al., 2020). In the cases where the coordinates do not precisely locate within the labelable volume in AAL3, the closest anatomical structure was judged by the authors.

Supplementary Table 1-A. Broad Function

cluster no.	size	p-val (cluster)	label	MNI coordinates x	y	z	T-Val	p-val (voxel)
1	684	1.25E-12	PHG, R	21	3	-30	7.035695	2.01E-12
			ATLsup, R	51	9	-12	6.021222	1.74E-09
			OFCpost, R	36	24	-27	5.896813	3.73E-09
2	406	3.91E-09	ATLmid, L	-36	12	-33	6.277258	3.48E-10
			Insula, L	-24	12	-18	4.90693	9.28E-07
			ATLsup, L	-45	6	-15	4.627445	3.71E-06
3	213	3.40E-06	SFGmedial, R	9	33	39	7.338632	2.20E-13
			SFG, R	15	42	57	4.457818	8.30E-06
4	193	7.57E-06	STG, L	-51	-18	3	5.851103	4.92E-09
			Insula, L	-33	-21	3	4.710975	2.47E-06
5	172	1.81E-05	Cerebellum, L	-18	-54	-66	7.491916	6.92E-14
			Cerebellum, R	3	-51	-66	4.80879	1.52E-06
6	104	0.0004064	MFG, R	36	27	39	6.198857	5.74E-10
7	97	0.0005793	OFCmed, L	-3	72	-3	6.416437	1.41E-10
8	80	0.0014226	Cerebellum, R	12	-93	-27	5.897382	3.72E-09

Supplementary Table 1-B. Mechanical Function

cluster no.	size	p-val (cluster)	label	MNI coordinates x	y	z	T-Val	p-val (voxel)
1	353	2.19E-08	MTG, L	-57	-3	-21	5.224254	1.76E-07
			PHG, L	-30	-3	-30	5.020742	5.17E-07
			OFCpost_L	-24	18	-21	4.765473	1.89E-06
2	234	1.50E-06	Cerebellum, L	-9	-54	-54	5.755369	8.70E-09
			Cerebellum, R	12	-54	-60	4.866502	1.14E-06
3	145	5.86E-05	ATLmid, R	57	12	-30	5.341671	9.26E-08
			ATLmid, R	39	-3	-27	4.518193	6.25E-06
4	132	0.0001059	MTG,L	-48	-36	-3	5.050767	4.42E-07
			OCCinf, L	-39	-60	-9	4.741597	2.13E-06
			ITG, L	-60	-48	-18	3.744445	0.000181
5	109	0.000317	CaudNuc. R	18	3	18	4.70877	2.50E-06
			thalamus, R	15	-21	12	4.242927	2.21E-05
6	95	0.000642	SMA, L	-6	24	66	4.900668	9.59E-07
7	86	0.0010291	ITG,R	42	-45	-9	5.254866	1.49E-07
8	60	0.0044661	Ptamen, R	27	-15	-6	4.624924	3.76E-06
9	55	0.0060587	Cerebellum, L	-33	-42	-42	4.661304	3.15E-06
10	51	0.0077847	PostCentral, R	18	-33	78	4.115608	3.87E-05
			SMA, R	9	-15	72	3.612443	0.0003037
11	48	0.0094357	SN, R	9	-9	-9	5.507887	3.65E-08

Supplementary Table 1-C. Motor Action

cluster no.	size	p-val (cluster)	label	MNI coordinates x	y	z	T-Val	p-val (voxel)
1	360	1.74E-08	SPL, R	27	-51	66	6.242261	4.35E-10
			AG, R	60	-66	33	5.464899	4.66E-08
			SPL, R	27	-69	63	5.126224	2.97E-07
2	328	5.10E-08	Precuneus, L	-18	-45	48	6.694631	2.19E-11
			Precuneus, R	12	-54	45	5.128943	2.93E-07
			CingulateMid, R	9	-24	39	4.996337	5.87E-07
3	228	1.89E-06	ATLinf, R	57	-15	-33	6.552504	5.72E-11
			ITG, R	45	-18	-15	4.797225	1.61E-06
4	157	3.45E-05	MFG, R	42	48	-6	6.203247	5.58E-10
5	145	5.86E-05	ATLinf, R	30	6	-48	9.301928	1.44E-20
6	100	0.0004971	OFCmed, L	-15	24	-18	6.723004	1.80E-11
			ATLsup, L	-21	12	-33	4.793944	1.64E-06
7	93	0.000712	SFG, L	-21	27	45	6.206962	5.45E-10
8	86	0.0010291	Cerebellum, R	24	-57	-30	5.062486	4.16E-07
			Cerebellum, R	39	-42	-30	4.858799	1.19E-06
9	77	0.0016777	Cerebellum, L	-48	-45	-45	6.156934	7.48E-10
			Cerebellum, L	-30	-42	-45	5.167318	2.39E-07
10	76	0.0017734	PreCentral, R	15	-15	78	5.796587	6.81E-09
11	57	0.0053572	Cerebellum, R	54	-63	-39	5.649143	1.62E-08
12	50	0.0082966	SPL, L	-18	-48	78	4.767743	1.87E-06

Supplementary Table 1-D. Object Structure

cluster no.	size	p-val (cluster)	label	MNI coordinates x	y	z	T-Val	p-val (voxel)
1	701	7.94E-13	OCCmid, L	-36	-78	0	10.11955	4.81E-24
			Fusiform, L	-36	-30	-27	6.557123	5.55E-11
			Lingual, L	-24	-63	-9	6.539894	6.22E-11
2	403	4.31E-09	Fusiform, R	33	-69	-3	7.547999	4.51E-14
			OCCmid, R	36	-69	27	7.218718	5.33E-13
3	270	3.93E-07	SMG, R	54	-33	42	7.911361	2.61E-15
			IPL, R	36	-45	51	6.253668	4.05E-10
4	164	2.55E-05	SFG, L	-24	0	45	8.479464	2.33E-17
			PreCentral, L	-42	3	45	6.734239	1.67E-11
			SMA, L	-9	-18	57	4.992063	6.00E-07
5	105	0.0003866	Insula, L	-30	21	0	6.701249	2.09E-11
6	98	0.0005504	PostCentral, R	18	-39	51	5.963926	2.48E-09
7	93	0.000712	MTG, R	48	-39	-9	6.563608	5.31E-11
8	91	0.0007903	STG, R	48	-54	21	7.118374	1.11E-12
9	87	0.0009758	SPL, L	-21	-57	42	7.238483	4.61E-13
10	58	0.0050402	ParsTri, R	57	39	15	5.137714	2.79E-07
11	52	0.0073075	ParsOper, L	-48	15	18	6.000751	1.98E-09
12	51	0.0077847	PreCentral, L	-33	-21	57	6.417862	1.40E-10

Supplementary Table 2. Conjunction across three models (broad/mechanical function, motor action)

cluster no.	size	p-val (cluster)	label	MNI coordinates x	y	z	T-Val	p-val (voxel)
1	146	5.603E-05	OFCpost, L	-24	21	-27	3.273167	0.0010643
			ATLinf, L	-42	6	-33	3.025974	0.0024798
			Putamen, L	-15	9	-12	2.501458	0.012372
2	88	0.0009254	Cerebellum, R	9	-51	-60	2.804335	0.0050443
3	73	0.0020974	ITG, R	57	-18	-24	3.382253	0.0007196
4	58	0.0050402	Putamen, R	36	-9	0	3.597909	0.0003211

Supplementary Table 3.

FeatureModels.xlsx: Bozeat's semantic features for the 90 common tools

REFERENCES

Bajada, C. J., Lambon Ralph, M. A., & Cloutman, L. L. (2015). Transport for language south of the Sylvian fissure: The routes and history of the main tracts and stations in the ventral language network. Cortex; a journal devoted to the study of the nervous system and behavior, 69, 141–151. https://doi.org/10.1016/j.cortex.2015.05.011

Binkofski, F., Dohle, C., Posse, S., Stephan, K. M., Hefter, H., Seitz, R. J., & Freund, H. J. (1998). Human anterior intraparietal area subserves prehension: a combined lesion and functional MRI activation study. Neurology, 50(5), 1253–1259. https://doi.org/10.1212/wnl.50.5.1253

Boronat, C. B., Buxbaum, L. J., Coslett, H. B., Tang, K., Saffran, E. M., Kimberg, D. Y., & Detre, J. A. (2005). Distinctions between manipulation and function knowledge of objects: evidence from functional magnetic resonance imaging. Brain research. Cognitive brain research, 23(2-3), 361–373. https://doi.org/10.1016/j.cogbrainres.2004.11.001

Bozeat, S., Lambon Ralph, M. A., Graham, K. S., Patterson, K., Wilkin, H., Rowland, J., Rogers, T. T., & Hodges, J. R. (2003). A duck with four legs: Investigating the structure of conceptual knowledge using picture drawing in semantic dementia. Cognitive neuropsychology, 20(1), 27–47. https://doi.org/10.1080/02643290244000176

Bozeat, S., Lambon Ralph, M. A., Patterson, K., & Hodges, J. R. (2002). When objects lose their meaning: what happens to their use?. Cognitive, affective & behavioral neuroscience, 2(3), 236–251. https://doi.org/10.3758/cabn.2.3.236

Buckner, R. L., Andrews-Hanna, J. R., & Schacter, D. L. (2008). The brain's default network: anatomy, function, and relevance to disease. Annals of the New York Academy of Sciences, 1124, 1–38. https://doi.org/10.1196/annals.1440.011

Buckner, R. L., & DiNicola, L. M. (2019). The brain's default network: updated anatomy, physiology and evolving insights. Nature reviews. Neuroscience, 20(10), 593–608. https://doi.org/10.1038/s41583-019-0212-7

Bullock, D. N., Hayday, E. A., Grier, M. D., Tang, W., Pestilli, F., & Heilbronner, S. R. (2022). A taxonomy of the brain's white matter: twenty-one major tracts for the 21st century. Cerebral cortex (New York, N.Y. : 1991), 32(20), 4524–4548. https://doi.org/10.1093/cercor/bhab500

Canessa, N., Borgo, F., Cappa, S. F., Perani, D., Falini, A., Buccino, G., Tettamanti, M., & Shallice, T. (2008). The different neural correlates of action and functional knowledge in semantic memory: an FMRI study. Cerebral cortex (New York, N.Y. :

1991), 18(4), 740–751. https://doi.org/10.1093/cercor/bhm110

Catani, M., Jones, D. K., Donato, R., & Ffytche, D. H. (2003). Occipito-temporal connections in the human brain. Brain : a journal of neurology, 126(Pt 9), 2093–2107. https://doi.org/10.1093/brain/awg203

Cavina-Pratesi, C., Connolly, J. D., & Milner, A. D. (2013). Optic ataxia as a model to investigate the role of the posterior parietal cortex in visually guided action: evidence from studies of patient M.H. Frontiers in human neuroscience, 7, 336. https://doi.org/10.3389/fnhum.2013.00336

Chen, L., Lambon Ralph, M. A., & Rogers, T. T. (2017). A unified model of human semantic knowledge and its disorders. Nature human behaviour, 1(3), 0039. https://doi.org/10.1038/s41562-016-0039

Coccia, M., Bartolini, M., Luzzi, S., Provinciali, L., & Ralph, M. A. (2004). Semantic memory is an amodal, dynamic system: Evidence from the interaction of naming and object use in semantic dementia. Cognitive neuropsychology, 21(5), 513–527. https://doi.org/10.1080/02643290342000113

Corbett, F., Jefferies, E., Burns, A., & Lambon Ralph, M. A. (2015). Deregulated semantic cognition contributes to object-use deficits in Alzheimer's disease: A comparison with semantic aphasia and semantic dementia. Journal of neuropsychology, 9(2), 219–241. https://doi.org/10.1111/jnp.12047

Corbett, F., Jefferies, E., Ehsan, S., & Lambon Ralph, M. A. (2009). Different impairments of semantic cognition in semantic dementia and semantic aphasia: evidence from the non-verbal domain. Brain : a journal of neurology, 132(Pt 9), 2593–2608. https://doi.org/10.1093/brain/awp146

Corbett, F., Jefferies, E., & Lambon Ralph, M. A. (2009). Exploring multimodal semantic control impairments in semantic aphasia: evidence from naturalistic object use. Neuropsychologia, 47(13), 2721–2731. https://doi.org/10.1016/j.neuropsychologia.2009.05.020

Corbett, F., Jefferies, E., & Lambon Ralph, M. A. (2011). Deregulated semantic cognition follows prefrontal and temporo-parietal damage: evidence from the impact of task constraint on nonverbal object use. Journal of cognitive neuroscience, 23(5), 1125–1135. https://doi.org/10.1162/jocn.2010.21539

Cox, C. R., Rogers, T. T., Shimotake, A., Kikuchi, T., Kunieda, T., Miyamoto, S., Takahashi, R., Matsumoto, R., Ikeda, A., Lambon Ralph, M. A. (2024). Representational similarity learning reveals a graded multidimensional semantic space in the human anterior temporal cortex. Imaging Neuroscience, 2, 1–22. doi: https://doi.org/10.1162/imag_a_00093

Ding, J., Chen, K., Liu, H., Huang, L., Chen, Y., Lv, Y., Yang, Q., Guo, Q., Han, Z., & Lambon Ralph, M. A. (2020). A unified neurocognitive model of semantics language social behaviour and face recognition in semantic dementia. Nature communications, 11(1), 2595. https://doi.org/10.1038/s41467-020-16089-9

Frisby, S. L., Halai, A. D., Cox, C. R., Lambon Ralph, M. A., & Rogers, T. T. (2023). Decoding semantic representations in mind and brain. Trends in cognitive sciences, 27(3), 258–281. https://doi.org/10.1016/j.tics.2022.12.006

Goldenberg, G., & Spatt, J. (2009). The neural basis of tool use. Brain : a journal of neurology, 132(Pt 6), 1645–1655. https://doi.org/10.1093/brain/awp080

Goldenberg, G., & Randerath, J. (2015). Shared neural substrates of apraxia and aphasia. Neuropsychologia, 75, 40–49. https://doi.org/10.1016/j.neuropsychologia.2015.05.017

Goodale, M. A., Króliczak, G., & Westwood, D. A. (2005). Dual routes to action: contributions of the dorsal and ventral streams to adaptive behavior. Progress in brain research, 149, 269–283. https://doi.org/10.1016/S0079-6123(05)49019-6

Goodale, M. A., & Milner, A. D. (1992). Separate visual pathways for perception and action. Trends in neurosciences, 15(1), 20–25. https://doi.org/10.1016/0166-2236(92)90344-8

Halai, A. D., Welbourne, S. R., Embleton, K., & Parkes, L. M. (2014). A comparison of dual gradient-echo and spin-echo fMRI of the inferior temporal lobe. Human brain mapping, 35(8), 4118–4128. https://doi.org/10.1002/hbm.22463

Hallam, G. P., Whitney, C., Hymers, M., Gouws, A. D., & Jefferies, E. (2016). Charting the effects of TMS with fMRI: Modulation of cortical recruitment within the distributed network supporting semantic control. Neuropsychologia, 93(Pt A), 40–52. https://doi.org/10.1016/j.neuropsychologia.2016.09.012

Herbet, G., Zemmoura, I., & Duffau, H. (2018). Functional Anatomy of the Inferior Longitudinal Fasciculus: From Historical Reports to Current Hypotheses. Frontiers in neuroanatomy, 12, 77. https://doi.org/10.3389/fnana.2018.00077

Hodges, J. R., Spatt, J., & Patterson, K. (1999). "What" and "how": evidence for the dissociation of object knowledge and mechanical problem-solving skills in the human brain. Proceedings of the National Academy of Sciences of the United States of America, 96(16), 9444–9448. https://doi.org/10.1073/pnas.96.16.9444

Hodges, J. R., Bozeat, S., Lambon Ralph, M. A., Patterson, K., & Spatt, J. (2000). The role of conceptual knowledge in object use evidence from semantic dementia. Brain : a journal of neurology, 123 (Pt 9), 1913–1925. https://doi.org/10.1093/brain/123.9.1913

Hodgson, V. J., Lambon Ralph, M. A., & Jackson, R. L. (2023). The cross-domain functional organization of posterior lateral temporal cortex: insights from ALE meta-analyses of 7 cognitive domains spanning 12,000 participants. Cerebral cortex (New York, N.Y. : 1991), 33(8), 4990–5006. https://doi.org/10.1093/cercor/bhac394

Humphreys, G. F., & Lambon Ralph, M. A. (2017). Mapping Domain-Selective and Counterpointed Domain-General Higher Cognitive Functions in the Lateral Parietal Cortex: Evidence from fMRI Comparisons of Difficulty-Varying Semantic Versus Visuo-Spatial Tasks, and Functional Connectivity Analyses. Cerebral cortex (New York, N.Y. : 1991), 27(8), 4199–4212. https://doi.org/10.1093/cercor/bhx107

Humphreys, G. F., Hoffman, P., Visser, M., Binney, R. J., & Lambon Ralph, M. A. (2015). Establishing task- and modality-dependent dissociations between the semantic and default mode networks. Proceedings of the National Academy of Sciences of the United States of America, 112(25), 7857–7862. https://doi.org/10.1073/pnas.1422760112

Ishibashi, R., Pobric, G., Saito, S., & Lambon Ralph, M. A. (2016). The neural network for tool-related cognition: An activation likelihood estimation meta-analysis of 70 neuroimaging contrasts. Cognitive neuropsychology, 33(3-4), 241–256. https://doi.org/10.1080/02643294.2016.1188798

Ishibashi, R., Lambon Ralph, M. A., Saito, S., & Pobric, G. (2011). Different roles of lateral anterior temporal lobe and inferior parietal lobule in coding function and manipulation tool knowledge: evidence from an rTMS study. Neuropsychologia, 49(5), 1128–1135. https://doi.org/10.1016/j.neuropsychologia.2011.01.004

Jackson, J.H. (1866). Remarks on those Cases of Disease of the Nervous System in which Defect of Expression is the most striking Symptom," Med. Times and Oaz., June 23, p. 659. As cited by Wilson S.A.K. 1908 A contribution to the study of apraxia with a review of the literature. Brain, 31, 164–216.

Jackson R. L. (2021). The neural correlates of semantic control revisited. NeuroImage, 224, 117444. https://doi.org/10.1016/j.neuroimage.2020.117444

Jackson, R. L., Cloutman, L. L., & Lambon Ralph, M. A. (2019). Exploring distinct default mode and semantic networks using a systematic ICA approach. Cortex; a journal devoted to the study of the nervous system and behavior, 113, 279–297. https://doi.org/10.1016/j.cortex.2018.12.019

Jackson, R. L., Rogers, T. T., & Lambon Ralph, M. A. (2021). Reverse-engineering the cortical architecture for controlled semantic cognition. Nature human behaviour, 5(6), 774–786. https://doi.org/10.1038/s41562-020-01034-z

Jarry, C., Osiurak, F., Delafuys, D., Chauviré, V., Etcharry-Bouyx, F., & Le Gall, D. (2013).

Apraxia of tool use: more evidence for the technical reasoning hypothesis. Cortex; a journal devoted to the study of the nervous system and behavior, 49(9), 2322–2333. https://doi.org/10.1016/j.cortex.2013.02.011

Jefferies E. (2013). The neural basis of semantic cognition: converging evidence from neuropsychology, neuroimaging and TMS. Cortex; a journal devoted to the study of the nervous system and behavior, 49(3), 611–625. https://doi.org/10.1016/j.cortex.2012.10.008

Jefferies, E., Hoffman, P., Jones, R., & Ralph, M. A. (2008). The impact of semantic impairment on verbal short-term memory in stroke aphasia and semantic dementia: A comparative study. Journal of memory and language, 58(1), 66–87. https://doi.org/10.1016/j.jml.2007.06.004

Jefferies, E., & Lambon Ralph, M. A. (2006). Semantic impairment in stroke aphasia versus semantic dementia: a case-series comparison. Brain : a journal of neurology, 129(Pt 8), 2132–2147. https://doi.org/10.1093/brain/awl153

Karnath, H. O., & Perenin, M. T. (2005). Cortical control of visually guided reaching: evidence from patients with optic ataxia. Cerebral cortex (New York, N.Y. : 1991), 15(10), 1561–1569. https://doi.org/10.1093/cercor/bhi034

Kriegeskorte N, Mur M, Bandettini P. Representational similarity analysis - connecting the branches of systems neuroscience. Front Syst Neurosci. 2008 Nov 24;2:4. doi: 10.3389/neuro.06.004.2008. PMID: 19104670; PMCID: PMC2605405.

Lambon Ralph, M. A., Jefferies, E., Patterson, K., & Rogers, T. T. (2017). The neural and computational bases of semantic cognition. Nature Reviews Neuroscience, 18(1), 42–55. https://doi.org/10.1038/nrn.2016.150

Lambon Ralph, M. A., Sage, K., Jones, R. W., & Mayberry, E. J. (2010). Coherent concepts are computed in the anterior temporal lobes. Proceedings of the National Academy of Sciences of the United States of America, 107(6), 2717–2722. https://doi.org/10.1073/pnas.0907307107

Lesourd, M., Servant, M., Baumard, J., Reynaud, E., Ecochard, C., Medjaoui, F. T., Bartolo, A., & Osiurak, F. (2021). Semantic and action tool knowledge in the brain: Identifying common and distinct networks. Neuropsychologia, 159, 107918. https://doi.org/10.1016/j.neuropsychologia.2021.107918

Liepmann, H. (1900). The syndrome of apraxia (motor asymbolia) based on a case of unilateral apraxia [Das Krankheitsbild der Apraxie ('motorischen Asymbolie') auf Grund eines Falles von einseitiger Apraxie.] Translated by Bohne WHO, Liepmann K, Rottenberg DA. from Monatsschrift für Psychiatrie und Neurologie, 1900, vol 8:15–44. In: Rottenberg DA, Hochberg FH. (eds). Neurological classics in modern

translation. New York: Hafner Press, 1977.

Makris, N., Preti, M. G., Wassermann, D., Rathi, Y., Papadimitriou, G. M., Yergatian, C., Dickerson, B. C., Shenton, M. E., & Kubicki, M. (2013). Human middle longitudinal fascicle: segregation and behavioral-clinical implications of two distinct fiber connections linking temporal pole and superior temporal gyrus with the angular gyrus or superior parietal lobule using multi-tensor tractography. Brain imaging and behavior, 7(3), 335–352. https://doi.org/10.1007/s11682-013-9235-2

Mesulam M. M. (2023). Temporopolar regions of the human brain. Brain : a journal of neurology, 146(1), 20–41. https://doi.org/10.1093/brain/awac339

Michalowski, B., Buchwald, M., Klichowski, M., Ras, M., & Kroliczak, G. (2022). Action goals and the praxis network: an fMRI study. Brain structure & function, 227(7), 2261–2284. https://doi.org/10.1007/s00429-022-02520-y

Menjot de Champfleur, N., Lima Maldonado, I., Moritz-Gasser, S., Machi, P., Le Bars, E., Bonafé, A., & Duffau, H. (2013). Middle longitudinal fasciculus delineation within language pathways: a diffusion tensor imaging study in human. European journal of radiology, 82(1), 151–157. https://doi.org/10.1016/j.ejrad.2012.05.034

Menon V. (2023). 20 years of the default mode network: A review and synthesis. Neuron, 111(16), 2469–2487. https://doi.org/10.1016/j.neuron.2023.04.023

Nili H, Wingfield C, Walther A, Su L, Marslen-Wilson W, Kriegeskorte N. A toolbox for representational similarity analysis. PLoS Comput Biol. 2014 Apr 17;10(4):e1003553. doi: 10.1371/journal.pcbi.1003553. PMID: 24743308; PMCID: PMC3990488.

Noonan, K. A., Jefferies, E., Visser, M., & Lambon Ralph, M. A. (2013). Going beyond inferior prefrontal involvement in semantic control: evidence for the additional contribution of dorsal angular gyrus and posterior middle temporal cortex. Journal of cognitive neuroscience, 25(11), 1824–1850. https://doi.org/10.1162/jocn_a_00442

Osiurak, F., & Badets, A. (2016). Tool use and affordance: Manipulation-based versus reasoning-based approaches. Psychological review, 123(5), 534–568. https://doi.org/10.1037/rev0000027

Patterson, K., Nestor, P. J., & Rogers, T. T. (2007). Where do you know what you know? The representation of semantic knowledge in the human brain. Nature reviews. Neuroscience, 8(12), 976–987. https://doi.org/10.1038/nrn2277

Pelgrims, B., Olivier, E., & Andres, M. (2011). Dissociation between manipulation and conceptual knowledge of object use in the supramarginalis gyrus. Human brain mapping, 32(11), 1802–1810. https://doi.org/10.1002/hbm.21149

Perenin, M. T., & Vighetto, A. (1988). Optic ataxia: a specific disruption in visuomotor

mechanisms. I. Different aspects of the deficit in reaching for objects. Brain : a journal of neurology, 111 (Pt 3), 643–674. https://doi.org/10.1093/brain/111.3.643

Phan, T. G., Donnan, G. A., Wright, P. M., & Reutens, D. C. (2005). A digital map of middle cerebral artery infarcts associated with middle cerebral artery trunk and branch occlusion. Stroke, 36(5), 986–991. https://doi.org/10.1161/01.STR.0000163087.66828.e9

Pobric, G., Jefferies, E., & Lambon Ralph, M. A. (2010). Category-specific versus category-general semantic impairment induced by transcranial magnetic stimulation. Current biology : CB, 20(10), 964–968. https://doi.org/10.1016/j.cub.2010.03.070

Poser, B. A., & Norris, D. G. (2009). Investigating the benefits of multi-echo EPI for fMRI at 7 T. NeuroImage, 45(4), 1162–1172. https://doi.org/10.1016/j.neuroimage.2009.01.007

Poser, B. A., Versluis, M. J., Hoogduin, J. M., & Norris, D. G. (2006). BOLD contrast sensitivity enhancement and artifact reduction with multiecho EPI: parallel-acquired inhomogeneity-desensitized fMRI. Magnetic resonance in medicine, 55(6), 1227–1235. https://doi.org/10.1002/mrm.20900

Ras, M., Wyrwa, M., Stachowiak, J., Buchwald, M., Nowik, A. M., & Kroliczak, G. (2022). Complex tools and motor-to-mechanical transformations. Scientific reports, 12(1), 8041. https://doi.org/10.1038/s41598-022-12142-3

Rice, G. E., Lambon Ralph, M. A., & Hoffman, P. (2015). The Roles of Left Versus Right Anterior Temporal Lobes in Conceptual Knowledge: An ALE Meta-analysis of 97 Functional Neuroimaging Studies. Cerebral cortex (New York, N.Y. : 1991), 25(11), 4374–4391. https://doi.org/10.1093/cercor/bhv024

Rouse, M. A., Binney, R. J., Patterson, K., Rowe, J. B., & Lambon Ralph, M. A. (2024). A neuroanatomical and cognitive model of impaired social behaviour in frontotemporal dementia. Brain : a journal of neurology, awae040. Advance online publication. https://doi.org/10.1093/brain/awae040

Saur, D., Kreher, B. W., Schnell, S., Kümmerer, D., Kellmeyer, P., Vry, M. S., Umarova, R., Musso, M., Glauche, V., Abel, S., Huber, W., Rijntjes, M., Hennig, J., & Weiller, C. (2008). Ventral and dorsal pathways for language. Proceedings of the National Academy of Sciences of the United States of America, 105(46), 18035–18040. https://doi.org/10.1073/pnas.0805234105

Schmahmann, J. D. & Pandya, D. (2009). Fiber Pathways of the Brain. Oxford Univ. Press.

Seltzer, B., & Pandya, D. N. (1984). Further observations on parieto-temporal connections in the rhesus monkey. Experimental brain research, 55(2), 301–312.

https://doi.org/10.1007/BF00237280
Shimotake, A., Matsumoto, R., Ueno, T., Kunieda, T., Saito, S., Hoffman, P., Kikuchi, T., Fukuyama, H., Miyamoto, S., Takahashi, R., Ikeda, A., & Lambon Ralph, M. A. (2015). Direct Exploration of the Role of the Ventral Anterior Temporal Lobe in Semantic Memory: Cortical Stimulation and Local Field Potential Evidence From Subdural Grid Electrodes. Cerebral cortex (New York, N.Y. : 1991), 25(10), 3802–3817. https://doi.org/10.1093/cercor/bhu262
Thompson, H. E., Noonan, K. A., Halai, A. D., Hoffman, P., Stampacchia, S., Hallam, G., Rice, G. E., De Dios Perez, B., Lambon Ralph, M. A., & Jefferies, E. (2022). Damage to temporoparietal cortex is sufficient for impaired semantic control. Cortex; a journal devoted to the study of the nervous system and behavior, 156, 71–85. https://doi.org/10.1016/j.cortex.2022.05.022
Tucciarelli, R., Wurm, M., Baccolo, E., & Lingnau, A. (2019). The representational space of observed actions. eLife, 8, e47686. https://doi.org/10.7554/eLife.47686
Tusa, R. J., & Ungerleider, L. G. (1985). The inferior longitudinal fasciculus: a reexamination in humans and monkeys. Annals of neurology, 18(5), 583–591. https://doi.org/10.1002/ana.410180512
Ueno, T., Saito, S., Saito, A., Tanida, Y., Patterson, K., & Lambon Ralph, M. A. (2014). Not lost in translation: generalization of the primary systems hypothesis to Japanese-specific language processes. Journal of cognitive neuroscience, 26(2), 433–446. https://doi.org/10.1162/jocn_a_00467
Valério, D., Santana, I., Aguiar de Sousa, D., Schu, G., Leal, G., Pavão Martins, I., & Almeida, J. (2021). Knowing how to do it or doing it? A double dissociation between tool-gesture production and tool-gesture knowledge. Cortex; a journal devoted to the study of the nervous system and behavior, 141, 449–464. https://doi.org/10.1016/j.cortex.2021.05.008
Visser, M., Jefferies, E., & Lambon Ralph, M. A. (2010). Semantic processing in the anterior temporal lobes: a meta-analysis of the functional neuroimaging literature. Journal of cognitive neuroscience, 22(6), 1083–1094. https://doi.org/10.1162/jocn.2009.21309
Wang, Y., Fernández-Miranda, J. C., Verstynen, T., Pathak, S., Schneider, W., & Yeh, F. C. (2013). Rethinking the role of the middle longitudinal fascicle in language and auditory pathways. Cerebral cortex (New York, N.Y. : 1991), 23(10), 2347–2356. https://doi.org/10.1093/cercor/bhs225
Weiller, C., Bormann, T., Saur, D., Musso, M., & Rijntjes, M. (2011). How the ventral pathway got lost: and what its recovery might mean. Brain and language, 118(1-2), 29–39.

https://doi.org/10.1016/j.bandl.2011.01.005

Whitney C, Kirk M, O'Sullivan J, Lambon Ralph MA, Jefferies E. The neural organization of semantic control: TMS evidence for a distributed network in left inferior frontal and posterior middle temporal gyrus. Cereb Cortex. 2011 May;21(5):1066-75. doi: 10.1093/cercor/bhq180. Epub 2010 Sep 17. PMID: 20851853; PMCID: PMC3077429.

Whitney, C., Kirk, M., O'Sullivan, J., Lambon Ralph, M. A., & Jefferies, E. (2012). Executive semantic processing is underpinned by a large-scale neural network: revealing the contribution of left prefrontal, posterior temporal, and parietal cortex to controlled retrieval and selection using TMS. Journal of cognitive neuroscience, 24(1), 133–147. https://doi.org/10.1162/jocn_a_00123

Zhao, Y., Halai, A. D., & Lambon Ralph, M. A. (2020). Evaluating the granularity and statistical structure of lesions and behaviour in post-stroke aphasia. Brain communications, 2(2), fcaa062. https://doi.org/10.1093/braincomms/fcaa062